Nonlinear Filtering for Ground Target Applications

Keith Kastella*, Chris Kreucher, Michael A. Pagels

Veridian ERIM International, Ann Arbor, MI

ABSTRACT

This paper describes a nonlinear filter for ground target tracking. Hospitability for maneuver derived from terrain, road and vehicle dynamics constraints is incorporated directly into the filter's motion model. The conditional probability density for the target state is maintained and updated with sensor measurements as soon as they become available. The conditional density is time updated between sensor measurements using finite difference methods. In simulations using square-law detected measurements the filter is able to track maneuvering ground targets when the Signal to Interference + Noise Ratio (SINR) is between 6 and 9 dB.

Keywords: Nonlinear filtering, ground moving target indicator, target tracking, Fokker-Planck Equation

1. INTRODUCTION

There is growing interest in ground target tracking, stimulated in large part by the success of JSTARS [1] and similar Ground Moving Target Indicator (GMTI) sensors [2]. Ground target Tracking differs from classical airborne and maritime tracking applications in that roads, terrain and other types of surface constraints are usually much more rigid than in the classical problems. These constraints constitute an additional information source and by including them in target motion models, tracking performance can be improved. A number of US Army programs have worked extensively to characterize vehicle motion preferences in terms of hospitability for maneuver and related factors. These preferences vary with position, weather, vehicle type (e.g. tracked vs. non-tracked) and mission. The work to date on incorporating such information into tracking filters has been based on variable structure interacting multiple models Kalman Filters (IMMKF) [7, 9]. These filters have spatially varying non-isotropic plant noise but do not directly incorporate dynamic vehicle inputs such as preferred heading or speed. For example, when driving on a road, drivers provide vehicle inputs (steering and accelerator) to align the vehicle axis with the road and maintain a preferred speed. The goal of the work reported here is to develop models of these control inputs and incorporate them directly into a nonlinear filter (NLF).

Another factor in GMTI tracking is that many missions require tracking vehicles that are moving beneath a forest canopy. In this case, the target Signal to Interference + Noise Ratio (SINR) is small. In such applications, NLF methods [3] may be particularly useful since the potential gain from improved target motion modeling increases as the SINR decreases. Furthermore, NLF can be used to process pre-thresholded data (i.e. – sensor pixel amplitudes) which does not suffer from any SINR loss due to thresholding [5,6].

This paper is organized as follows. Section 2 describes briefly how terrain analysis is used to obtain hospitability maps. Section 3 synopsizes NLF and develops target motion models derived from Hospitability for Maneuver (HM). The Fokker-Planck equation (FPE) needed to characterize the time-evolution of the conditional target state probability density in an NLF is then obtained. The FPE is solved numerically using Alternating Direction Implicit (ADI) finite difference methods [5,6,8,10,14]. This forms the basis of a nonlinear filter that incorporates both hospitability and envelope detected (pre-thresholded) sensor measurements. A method for developing the target motion models directly from vehicle motions themselves is presented in Section 4. Section 5 presents a few preliminary results indicating that with this approach, target tracking is feasible for maneuvering targets at about 6-9 dB SINR.

2. HOSPITABILITY ANALYSIS

As part of the preparation of battlefield intelligence, terrain analysis is performed to capture the effects that Hospitability for Maneuver (HM) and hospitability for emplacement can have on battle outcomes. In maneuver planning existing lines of communication may be inappropriate, requiring cross-country movement.

* Correspondence: Email: Kastella@ERIM-Int.com; Telephone: (734) 994-1200 x 2283; Fax: (734) 994-5905; Mail: Veridian ERIM International, P. O. Box 134008, Ann Arbor, MI 48113-4008.

In *Signal and Data Processing of Small Targets 2000*, Oliver E. Drummond, Editor, Proceedings of SPIE Vol. 4048 (2000) • 0277-786X/00/$15.00

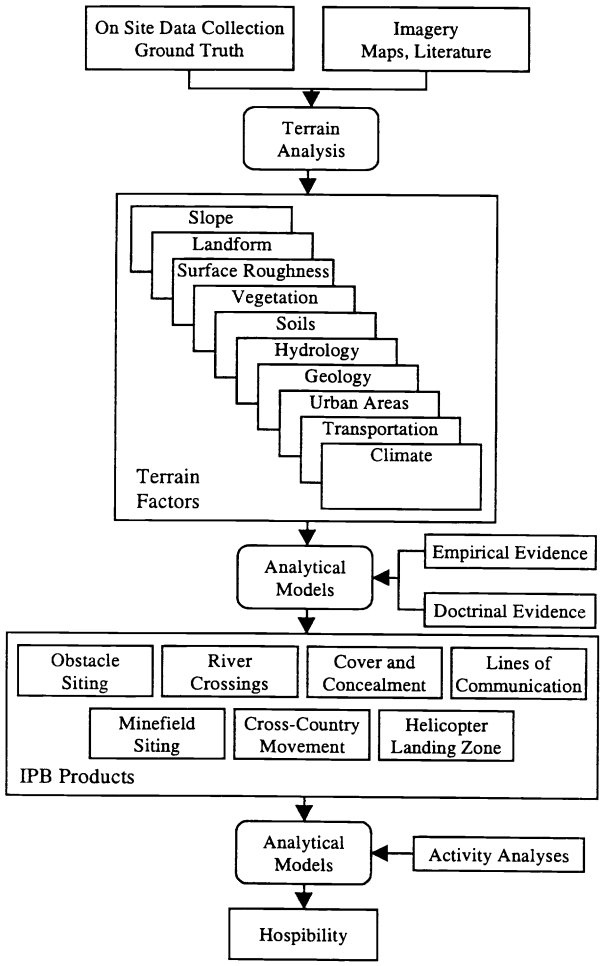

Figure 1: Data Flow in a Classic Terrain Analysis Procedure

Figure 1 details the data flow for terrain analysis with the addition of an activity product. Terrain analysis begins with the raw terrain data extracted from imagery, maps, literature, or data collected during on-site inspections. These data are analyzed and reduced to a set of terrain factor products capturing important terrain features and classifications [11]. This portion of the analysis is usually automated and is described in more detail in publicly available USGS and NIMA products. The next step in the terrain analysis procedure is to combine terrain factor products with empirical and doctrinal evidence to generate complex products capturing activities of military significance [12]. For example, cross-country movement incorporates terrain factors such as slope, landform, surface roughness, vegetation, and soils. These factors are combined with analytical models [13] which capture the capabilities of specific vehicles (usually empirically derived), to produce a maximum vehicle speed in a given area.

The generation of activity specific products is an advance over classical terrain analysis and intelligence preparation procedures. These products capture interactions between activity requirements such as a need for long-term hide site and constraints or opportunities provided by local terrain. For maneuver-like activities, hospitability provides a measure of the support a given local area provides for a given activity. Hospitability has been successfully utilized in both DARPA and NIMA imagery exploitation systems, and has had particular success when applied to the identification of mobile missiles.

Tuning of the analytical models within this process is accomplished primarily in two ways: application of physical constraints, and the analysis of vehicle tracks. For example, the physical limitations of the M1A1 tank (e.g., maximum traversable slope, surface roughness vs. speed effects) are directly incorporated into the analytical models. Vehicle track analysis provides exactly the terrain over which certain vehicles travel. While not excluding any terrain combination, it can be analyzed to provide preferences and as a test of the physical vehicle constraint derived model parameters.

An example of hospitability for maneuver obtained from the Terrain Delimitation component of DARPA's Semi-Automated IMINT Processing (SAIP) system is shown in Figure 2. The geographic area is the National Training Center (NTC), Ft. Irwin CA. It's source data included products from the USGS and NIMA.

3. NONLINEAR FILTERING

The structure of NLF is similar to that of a conventional Kalman filter in that it consists of 1) measurement update and 2) time update or prediction. NLF differs from the Kalman filter in that is develops an estimate of the entire target state conditional density (for a detailed exposition, see [6]). In contrast, the Kalman filter is based on an estimate of the first two moments of the conditional density. To track a moving ground target from a sequence of measurements $\mathbf{y}_k$ made at discrete

times t_k, we must develop a statistical model of the target motion that incorporates hospitability for maneuver (HM). In filtering applications, target dynamics are described by the Ito stochastic differential equation for the time-dependent target state $\mathbf{x}_t$

$$d\mathbf{x}_t = \mathbf{f}(\mathbf{x}_t, t)dt + \mathbf{G}(\mathbf{x}_t, t)d\beta_t, \quad t \geq t_0 \tag{1}$$

where $\mathbf{x}_t$ and $\mathbf{f}$ are n-vectors, $\mathbf{G}$ is an $n \times r$ matrix function and $\{\beta_t, t \geq t_0\}$ is an r-vector Brownian motion process with $E\{d\beta_t d\beta_t^{\mathrm{T}}\} = \mathbf{Q}(t)dt$.

The observations up to time t are denoted $Y_t = \{\mathbf{y}_k : t_k \leq t\}$. In nonlinear filtering, the target state conditional probability density function $p(\mathbf{x}_t \mid Y_t)$ is constructed recursively. Given a new observation $\mathbf{y}_k$, the updated conditional density $p(\mathbf{x}_{t_k} \mid Y_{t_k})$ is obtained from the predicted density $p(\mathbf{x}_{t_k} \mid Y_{t_{k-1}})$ using Bayes' formula:

$$p(\mathbf{x}_{t_k} \mid Y_{t_k}) = \frac{p(\mathbf{y}_k \mid \mathbf{x}_{t_k}) p(\mathbf{x}_{t_k} \mid Y_{t_{k-1}})}{\int d\mathbf{x}'_{t_k} p(\mathbf{y}_k \mid \mathbf{x}'_{t_k}) p(\mathbf{x}'_{t_k} \mid Y_{t_{k-1}})} \tag{2}$$

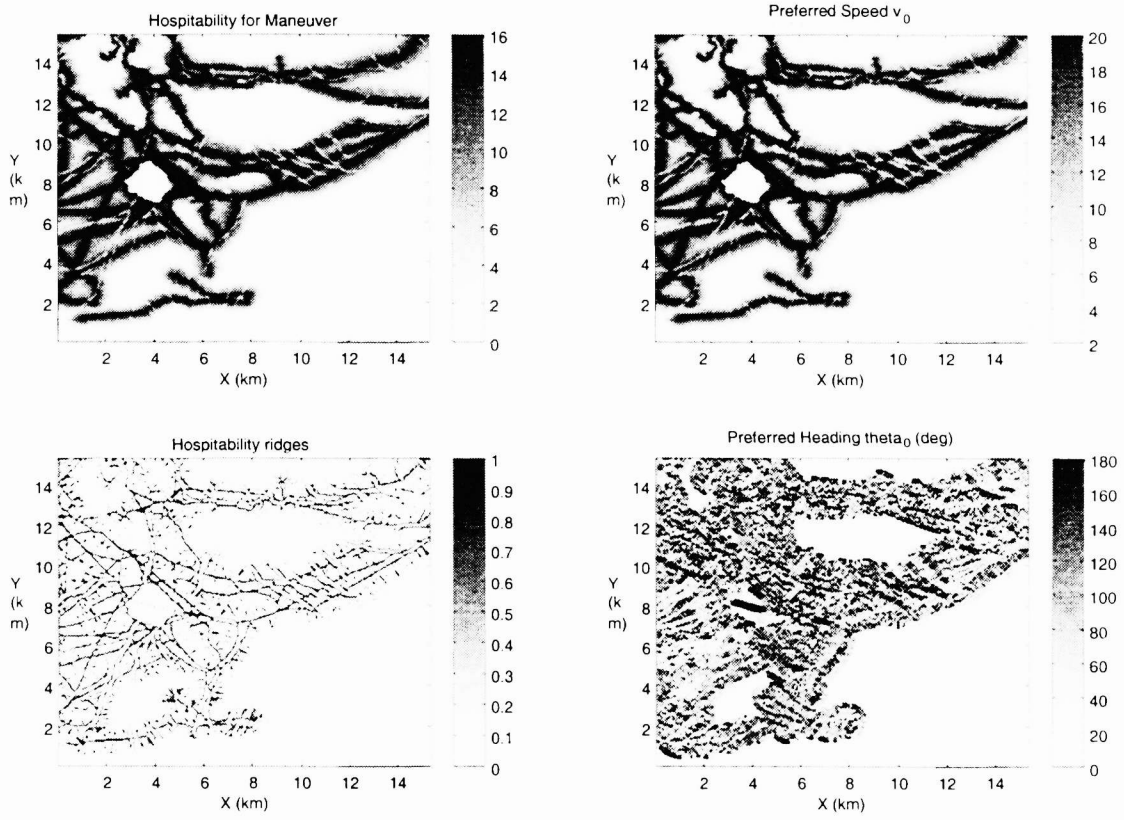

Figure 2 – Hospitability for maneuver (HM) (upper left), preferred speed (m/s) (upper right), hospitability ridges (lower left) and preferred heading (lower right) for a 14 km x 14 km region of the National Training Center (NTC) near Ft. Irwin, CA.

where the measurement likelihood $p(\mathbf{y}_k \mid \mathbf{x}_{t_{k_C}})$ is given by a physical sensor model. Then the minimum mean square error target state estimate $\hat{\mathbf{x}}_{t_k}$ at time t_k is

$$\hat{\mathbf{x}}_{t_k} = \int d\mathbf{x}_{t_k} \mathbf{x}_{t_k} p(\mathbf{x}_{t_k} \mid Y_{t_k}), \tag{3}$$

with covariance

$$\Sigma = \int d\mathbf{x}_{t_k} \left(\hat{\mathbf{x}}_{t_k} - \mathbf{x}_{t_k}\right)\left(\hat{\mathbf{x}}_{t_k} - \mathbf{x}_{t_k}\right)^{\mathrm{T}} p(\mathbf{x}_{t_k} \mid Y_{t_k}). \tag{4}$$

Between observations the evolution of the conditional density is determined by the target dynamics as characterized by the Ito equation. Between measurements the time evolution of the conditional density is the solution to the Fokker-Planck equation (FPE)

$$\frac{\partial p}{\partial t}(\mathbf{x}_t \mid Y_{t_k}) = L\left(p(\mathbf{x}_t \mid Y_{t_k})\right), \quad t_k \le t < t_{k+1}, \tag{5}$$

where

$$L(p) \equiv -\sum_{i=1}^{n} \frac{\partial(\mathbf{f}_i p)}{\partial \mathbf{x}_i} + \frac{1}{2}\sum_{i,j=1}^{n} \frac{\partial^2\left(p\left(\mathbf{G}\mathbf{Q}\mathbf{G}^{\mathrm{T}}\right)_{ij}\right)}{\partial \mathbf{x}_i \partial \mathbf{x}_j} \tag{6}$$

with initial condition given by $p(\mathbf{x}, t_k \mid Y_{t_k})$.

3.1 Target Motion Models and Hospitability for Maneuver

To develop a filter incorporating HM into the target motion model, the target state is modeled using the 4-dimensional state

$$\mathbf{x} = (x, y, \theta, v)^{\mathrm{T}} \tag{7}$$

where x and y are the target's Cartesian location in the topocentric plane (meters) centered on the region of interest, θ is the target heading and v is the target speed (m/s).

Ito equations that couple the target dynamics to the spatially varying HM can be constructed using Inhomogenous Integrated Ornstein-Uhlenbeck (IIOU) models. HM represents a spatially varying preferred target speed, $v_0(x, y)$, shown in the Figure 2. If the mean time to correct speed variations is τ_v (which can vary with location), then the IIOU model is

$$dv = -\frac{1}{\tau_v}\left(v - v_0(x, y)\right)dt + d\beta_v \tag{8}$$

where $d\beta_v$ is a white Brownian motion process with power spectral density $E\left(d\beta_v^{\,2}\right) = q_v dt$ where $q_v = \frac{2}{\tau_v}\sigma_v^2$ and σ_v^2 is the variance of the speed deviation from its preferred value.

To develop a model of heading dynamics we assume that targets prefer to follow regions of high HM. This corresponds to following the hospitability ridges shown in the lower left portion of Figure 2. The preferred heading tends to be either

parallel or anti-parallel to the HM ridge axis $\varphi(x, y)$ (shown in the lower right portion of Figure 2). This means that the preferred heading at each location is two-valued. When the current target heading is within 90° of the ridge axis, the target will maneuver to align its heading with the ridge. If the deviation between the ridge axis and the target heading is greater than 90°, then the preferred target heading will be anti-parallel to the ridge axis. This is captured by the Ito equation

$$d\theta = -\frac{1}{\tau_\theta}(\theta - \theta_0(x, y, \theta))dt + d\beta_\theta \qquad (9)$$

where the preferred heading is

$$\theta_0(x, y, \theta) = \begin{cases} \varphi(x, y), & |\theta - \varphi(x, y)| < \pi/2 \\ \varphi(x, y) + \pi, & \text{otherwise,} \end{cases} \qquad (10)$$

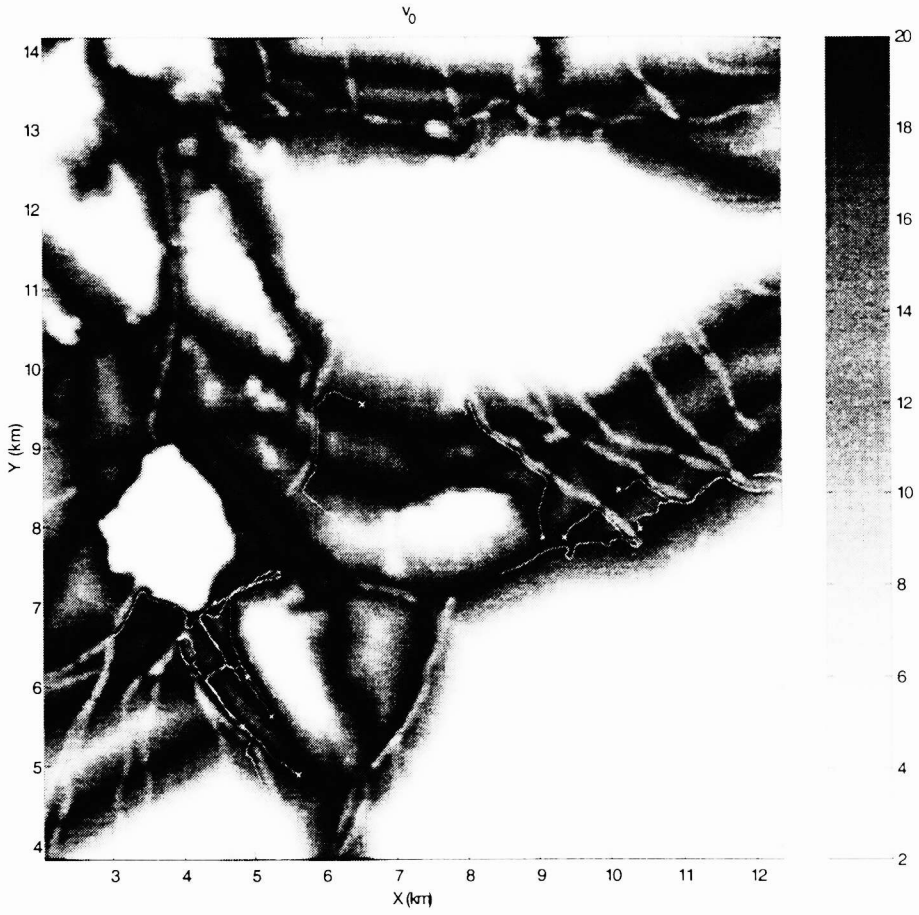

Figure 3 – Several simulated vehicle trajectories (solid white lines), overlain on the preferred speed v_0 (m/s), derived from the HM of Figure 2, obtained as numerical solutions to the target state Eq. (7) with Ito equations (8) and (9) for the spatially varying preferred heading and speed. The start of each trajectory is indicated by an asterisk.

where angle differences are calculated modulo 2π. The power spectral density of the heading process is $E\left(d\beta_\theta{}^2\right) = q_\theta dt$ where $q_\theta = \frac{2}{\tau_\theta}\sigma_\theta^2$.

Defining $\dot{x} = v\cos(\theta)$ and $\dot{y} = v\sin(\theta)$, the FPE (Eq. (5)) becomes

$$\frac{\partial p}{\partial t} = -\dot{x}\frac{\partial p}{\partial x} - \dot{y}\frac{\partial p}{\partial y} + \frac{1}{\tau_\theta}\frac{\partial}{\partial \theta}\left((\theta - \theta_0(x,y,\theta))p\right) + \frac{1}{\tau_v}\frac{\partial}{\partial v}\left((v - v_0(x,y))p\right) + \frac{1}{2}q_\theta\frac{\partial^2 p}{\partial \theta^2} + \frac{1}{2}q_v\frac{\partial^2 p}{\partial v^2} \tag{11}$$

3.2 The Measurement Model

We model the target measurements as square-law detected return amplitude on a uniform grid of size $M = N_x \times N_y$ (for simplicity, we ignore the usual Doppler estimate obtained as part of the GMTI measurement). The amplitude in pixel i for scan k is $y_{k,i}$ and the entire scan is $\mathbf{y}_k = \{y_{k,i} \mid i = 1,\ldots,M\}$. Let $i_\mathbf{x}$ denote the target-containing pixel. For a target with SINR λ (here assumed known), the probability distribution for the amplitude in pixel $i_\mathbf{x}$ is

$$p_1(y_{i_\mathbf{x}}) = \frac{1}{1+\lambda}\exp\left(-y_{i_\mathbf{x}}/(1+\lambda)\right). \tag{12}$$

The distribution in the empty cells is $p_0(y_{i_\mathbf{x}}) = \exp\left(-y_{i_\mathbf{x}}\right)$. The density for the entire scan is

$$p(\mathbf{y}_k \mid \mathbf{x}_k) = \kappa\, p_1(y_{k,i_\mathbf{x}}) / p_0(y_{k,i_\mathbf{x}}) \tag{13}$$

where κ is a target-state independent constant that can be discarded in the Bayes' formula update.

4. DERIVING IIOU PARAMETERS FROM TARGET MOTION DATA

This section details an approach to deriving IIOU parameters directly from observed target motion rather than HM. Truth data based on GPS measurements of the vehicle positions over time has been collected as part of the battle training at NTC. This data can be used to directly estimate the IIOU parameters for a region of interest. This has the advantage motion model parameters can be quantitatively inferred. The disadvantage of this approach is that, in wartime, vehicles will often need to be tracked in areas where they have not previously been observed. In such cases, the methods of terrain analysis described in Section 2 are required.

The discrete time Ito equation for vehicle speed corresponding to Eq. (8) is

$$v^{k+1} = v^k - \frac{\Delta t}{\tau_v(x,y)}\left[v^k - v_0(x,y)\right] + \sqrt{q_v(x,y)\Delta t}\; w^{k+1} \tag{14}$$

where v^k is the speed at time k, $v_o(x,y)$ is the preferred speed at x, y, $\tau_v(x,y)$ is the time constant and $q_v(x,y)$ is the magnitude of the power spectral density and w^{k+1} is unit variance zero mean Gaussian noise. Note that we allow τ_v and q_v to vary with position here.

We estimate parameters $v_o(x,y)$, $\tau_v(x,y)$ and $q_v(x,y)$ using movement data consisting of vehicle positions (x_k, y_k) at times t_k for a collection of vehicles on training maneuvers at NTC as follows. For each vehicle, the speed at a point (x_k, y_k) is computed using forward differencing

$$v^k = \frac{\sqrt{(x^{k+1} - x^k)^2 + (y^{k+1} - y^k)^2}}{(t^{k+1} - t^k)} \tag{15}$$

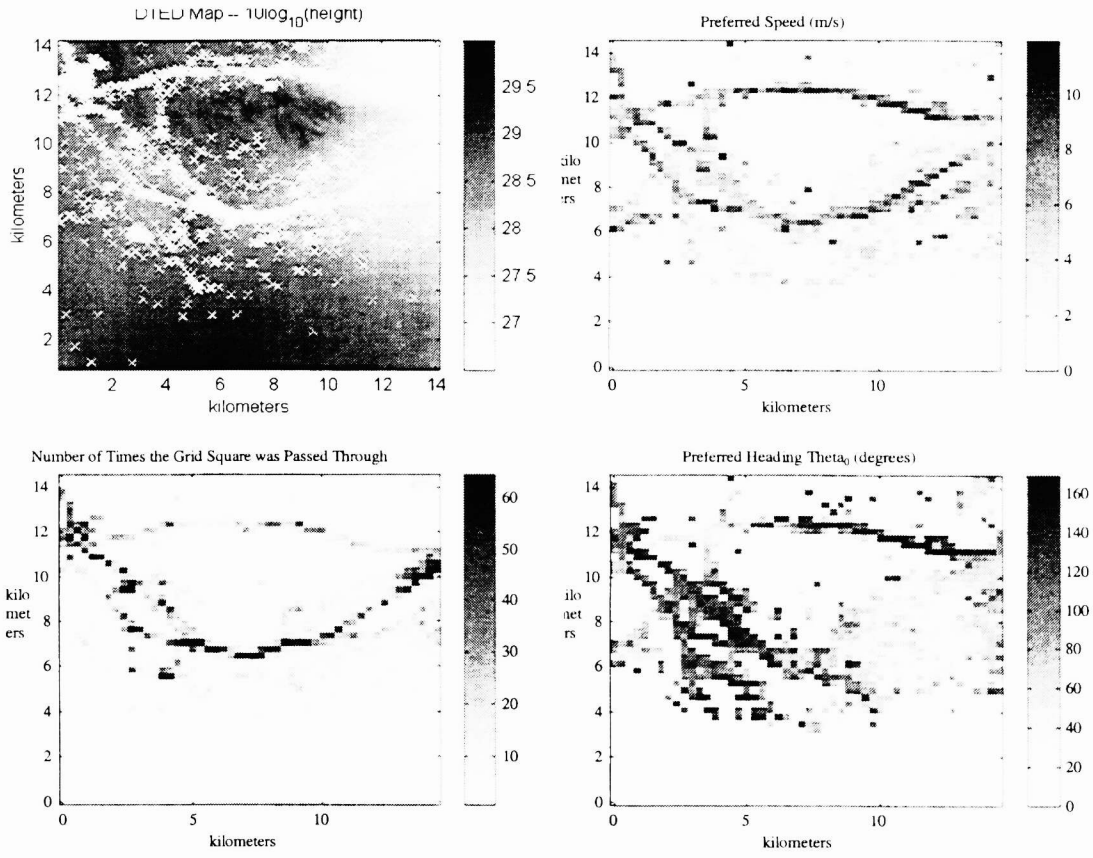

Figure 4—Vehicle locations (x) overlain on DTED (upper left) for an exercise at NTC. These are used to compute the preferred speed (upper right), number of times vehicles pass each subregions of the terrain (lower left) and the preferred heading (lower right). Note the similarity between these plots and the HM-derived speed and heading preferences of Figure 2.

The speed v^k is associated with the point (x_k, y_k) and the time t_k. The preferred vehicle speed at a point, $v_o(x, y)$, can be estimated using a simple averaging technique:

$$\hat{v}_0(x_k, y_k) = \frac{v^{k-1} + v^k + v^{k+1}}{3} \tag{16}$$

To obtain the time constant $\tau_v(x, y)$ define the residual difference between the true speed and the preferred speed as $\tilde{v}^k = v^k - v_0$. Then the residual obeys the Ito equation for a *homogenous* Ornstein-Uhlenbeck process,

$$\tilde{v}^{k+1} = \tilde{v}^k - \frac{\Delta t}{\tau_v(x, y)}\tilde{v}^k + \sqrt{q_v(x, y)\Delta t}\, w^{k+1} \tag{17}$$

Evaluating expected values we find,

$$\left\langle \tilde{v}^{k+1}\tilde{v}^k \right\rangle = \left\langle \tilde{v}^k\tilde{v}^k \right\rangle - \left\langle \frac{\Delta t}{\tau_v(x, y)}\tilde{v}^k\tilde{v}^k \right\rangle + \left\langle \sqrt{q_v(x, y)\Delta t}\, w^{k+1}\tilde{v}^k \right\rangle \tag{18}$$

$$\left\langle \tilde{v}^{k+1}\tilde{v}^k \right\rangle = \left[1 - \frac{\Delta t}{\tau_v(x, y)}\right]\left\langle \tilde{v}^k\tilde{v}^k \right\rangle \tag{19}$$

where $\langle\cdot\rangle$ denotes expectation over the ensemble. Since $\tilde{v}^k$ and w^{k+1} are uncorrelated and have mean 0, we may solve for $\tau_v(x, y)$ to obtain $\tau_v(x, y) = 2\Delta t\left\langle \tilde{v}^k\tilde{v}^k \right\rangle / \left\langle \left(\tilde{v}^{k+1} - \tilde{v}^k\right)^2 \right\rangle$. This is approximated using a three-term sum

$$\hat{\tau}_v(x, y) \approx \frac{2\Delta t}{3}\frac{\sum_{i=k-1}^{i=k+1}\left(\tilde{v}^i\right)^2}{\sum_{i=k-1}^{i=k+1}\left(\tilde{v}^{i+1} - \tilde{v}^i\right)^2} \tag{20}$$

To estimate $q_v(x, y)$ we note that

$$q_v(x, y)\left(w^{k+1}\right)^2 = \frac{1}{\Delta t}\left\{\left[\tilde{v}^{k+1} - \left(1 - \frac{\Delta t}{\tau_v(x, y)}\right)\tilde{v}^k\right]\right\}^2 \tag{21}$$

since w^{k+1} has unit variance, $q_v(x, y) = \frac{1}{\Delta t}\left\langle \left[\tilde{v}^{k+1} - \left(1 - \frac{\Delta t}{\tau_v(x, y)}\right)\tilde{v}^k\right]^2 \right\rangle$ and

$$\hat{q}_v(x,y) \approx \frac{1}{3\Delta t}\sum_{i=k-1}^{i=k+1}\left[\tilde{v}^{i+1} - \left(1 - \frac{1}{t_v(x,y)}\right)\tilde{v}^{i}\right]^2 \tag{22}$$

Similar reasoning can be applied to estimate the heading parameters $\theta_o(x,y)$, $\tau_\theta(x,y)$ and $q_\theta(x,y)$. Once the relevant parameters have been estimated for all of the vehicles in the area of interest, we create a series of spatial grids to hold the averages of each parameter.

5. RESULTS

Algorithms to extract preferred speed and heading from HM have been implemented in MatLab. Figure 2 shows HM, the preferred speed derived from it, HM ridges and the preferred heading. (Here the preferred speed is defined to be an affine transformation of the HM). Figure 3 shows several simulated target trajectories obtained by solving the Ito equation (8) and (9) for the target state (7). These trajectories use the HM-derived IIOU parameters with randomly selected starting points on the HM ridges. The time constants and standard deviations are constant with $\tau_v = \tau_\theta = 1$ s, $\sigma_v = 1$ m/s and $\sigma_\theta = 1^\circ$.

Figure 4 shows the result of IIOU parameter estimation obtained directly from the NTC data using the method described in Section 4. Note the marked similarity between the HM-derived and NTC-derived IIOU parameters. However, the HM-derived parameters are available over the entire region while the NTC-derived parameters are only available in areas where vehicles have been observed in the past. Also, the resolution of the NTC-derived parameters is much coarser, due to

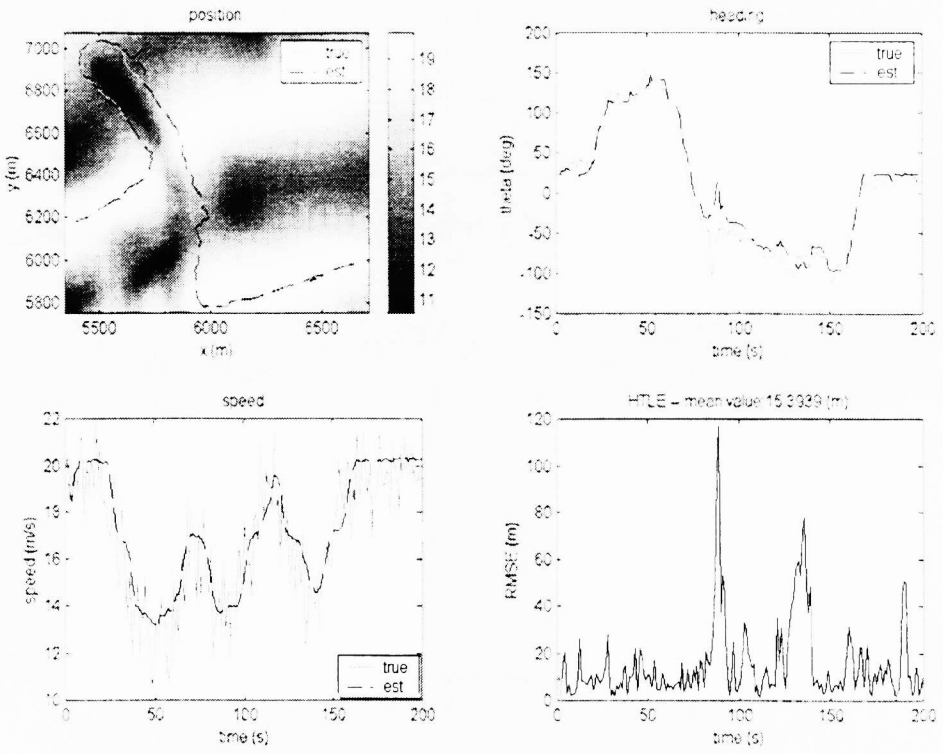

Figure 5 – Tracking results using NLF. The target SINR is 6 dB. The true and estimate tracks are shown at upper left. The heading and speed are shown at upper right and lower left. The Horizontal Track Location Error (HTLE) is plotted at lower right. The RMS error is about 15 m.

limitations in the statistical resolution.

Numerical Fokker-Planck equation solver and measurement models were also implemented in MatLab. A simulated trajectory and the trajectory estimate are shown in Figure 5. A variant of the Alternating Direction Implicit (ADI) method detailed in [5,6,8,10] was used to solve FPE between measurement updates. The ADI solver is a finite difference method that discretizes the FPE on a grid of size $N = N_x \times N_y \times N_v \times N_\theta$. The grid size was $N_x = N_y = 19$, $N_v = N_\theta = 5$ so $N = 9025$. The resolution of the grid was $\Delta x = \Delta y = 15$ m, $\Delta\theta = 30^\circ$ and $\Delta v = 3$ 1/3 m/s. The SINR is very low, $\lambda = 4$ (i.e. $10\log_{10}\lambda = 6$ dB). Measurements are generated on a 1 s interval. The grid is translated to remain centered on the estimated target location, heading and speed. The spatial resolution of the sensor (i.e. the pixel size) was 15m $\times$ 15m (no Doppler measurement was assumed). The RMS Horizontal Track Location Error (HTLE) is about 15 m. It is interesting to note that where the peak error occurs at t = 80 s (presumably due to several low amplitude measurements), the target is traversing a hospitability neck. Here the constrained hospitability helps the filter recover and regain lock on the target. Based on very limited Monte Carlo testing, the RMS HTLE is on the order of 10 m at 9 dB SINR and about 20 m at 6 dB SINR. The mean track lifetime (i.e. the amount of time the filter can keep the target on the FPE grid) is 10's of minutes at 9 dB and a few minutes at 6 dB.

6. ACKNOWLEDGEMENT

The authors benefited from discussions with James Gleason, Stan Musick, Nikola Subotic and Barton Yeary. This work was sponsored by Veridian ERIM International under its internal research and development program and by the Air Force Research Laboratory under contract SPO900-96-D-0080.

7. REFERENCES

1. J. N Entzminger, Jr., C A. Fowler, W. J. Kenneally, "JointSTARS and GMTI: Past, Present and Future", IEEE Trans. AES, Vol 35, No. 2, Apr, '99, pp. 748-760.

2. L. A. Gross, R. A. Guarino, H. D. Holt, Jr., "AN/APY-6 Real Time Surveillance and Targeting Radar Development", RTO SET Symposium on "High Resolution Radar Techniques", Granada, Spain, 22-24 March, 1999, RTO-MP-40, pp. 31.1-31.6.

3. Y. C. Ho, R. C. K. Lee, "A Bayesian Approach to Problems in Stochastic Estimation and Control", *IEEE Trans. Auto. Cont.*, Vol. 19, Oct., 1964, pp. 333-339.

4. A. H. Jazwinski, 1970, *Stochastic Processes and Filtering Theory*, Academic Press, New York.

5. K. Kastella and A. Zatezalo, "Nonlinear Filtering for Low Elevation Targets in the Presence of Multipath Propagation", *Proceedings of SPIE Aerosense '98*, Signal and Data Processing of Small Targets 1998, Vol. 3373, pp. 452-459.

6. K. Kastella , " Finite Difference Methods for Nonlinear Filtering and Automatic Target Recognition ", in *Multitarget / Multisensor Tracking: Applications and Advances Volume III*, Y. Bar-Shalom and W. D. Blair (ed.), Artech House, Dedham MA, 2000.

7. T. Kirubarajan, Y. Bar-Shalom, K. R. Pattipati, I. Kadar, "Ground Target Tracking with Variable Structure IMM Estimator", *IEEE AES* Jan, '00, Vol 36, No. 1, pp. 26-46.

8. W. H. Press, S. A Teukolsky, W. T. Vetterling, B. P. Flannery, *Numerical Recipes in C - Second Edition*, (1992), Cambridge University Press.

9. P. J. Shea, T. Zadra, D. Klamer, E. Frangione, R. Brouillard, K. Kastella, "Precision Tracking of Ground Targets", in *Proceedings of the IEEE Aerospace Conference*, Big Sky, MT, March 18-25, 2000.

10. J. C. Strikwerda, *Finite Difference Schemes and Partial Differential Equations*, Chapman & Hall, New York, 1989.

11. US Army Material Systems Analysis Activity, "The Natick landform classification system," in *Tec. Re*p. 100, vol . October, Aberdeen Proving Ground, MD: US Army, 1974.

12. US Army Corp of Engineers, *Terrain analysis procedural guide for surface configuration.* Fort Belvoir, VA: Engineering Topographic Laboratories, 1984.

13. US Army Corp of Engineers, "Stochastic vehicle mobility forecasts using the NATO reference mobility model," Department of the Army, Washington, DC GL-92-11, 1992.

14. Zatezalo, *Tracking and Detection for the Target State Model*, University of Minnesota M. S. Thesis, March 15, 1997.